Extracting Meaningful Information from Uncalibrated Backscattered Echo Intensity Data

Louis Gostiaux

Laboratoire des Écoulements Géophysiques et Industriels, CNRS UMR 5519, Grenoble, France

Hans van Haren

Royal Netherlands Institute for Sea Research, Den Burg, Netherlands

(Manuscript received 30 March 2009, in final form 17 September 2009)

ABSTRACT

The authors present an original method for the analysis of acoustic Doppler current profiler (ADCP) echo intensity profiles measured in the ocean, especially when no calibration has been performed. This study is based on data from Teledyne RD Instrument acoustic profilers but provides a methodology that can be extended to other kinds of hardware. To correctly interpret data for which the signal-to-noise ratio is below a factor of 10, the authors propose isolating the backscattered signal from noise in arithmetic space before resolving the sonar equation and compensating for transmission loss in logarithmic space. The robustness of the method is shown for several independent datasets from the Atlantic Ocean, the North Sea, and the Mediterranean Sea. Estimation of sediment concentration, planktonic migrations, or air bubbles is now possible at less than 10 dB above noise level, which can concern half of the ADCP's range under common circumstances.

1. Introduction

Acoustic Doppler current profiler (ADCP) echo intensity data are usually recorded as a by-product of the velocity measurements. Echo intensity reflects the backscattering strength of the water, which is due to the presence of backscatterers such as solid particles, bubbles, or living organisms. The level of echo intensity is also very dependent on the acoustic frequency of the ADCP, because the ratio between the acoustic wavelength and the size of the scatterers partially governs the backscattering strength. These data can provide useful information on sediment transport (Gartner 2004; Wall et al. 2006), plankton activity (Plueddemann and Pinkel 1989), or surface wave field intensity (Zedel 2001). In physical oceanography, the displacement of the scatterers advected by the flow helps in visualizing the flow structure (van Haren 2009). Moreover, by taking advantage of the angular separation between the (four) different beams of the ADCP, additional information on the flow can be obtained that infers direction of fronts or any other nonlinear structure (van Haren 2007a).

To be related to pertinent physical quantities, the backscattered signal needs to be calibrated by means of extra sensors that measure independently the quantity one wants to relate to echo intensity, such as sediment concentration and grain-size distribution or plankton activity. This is done by means of water sampling (Wall et al. 2006), sediment traps, or nets (Flagg and Smith 1989). Optical backscatter sensors (OBS) can also be used, because their calibration can easily be performed in the laboratory using the above-mentioned water samples (Kim and Voulgaris 2003). The calibration of profiling acoustic devices in the laboratory is more complex, because a large volume of fluid has do be ensonified. It can be performed successfully for short-range acoustic backscatter devices (Betteridge et al. 2008) but not for long-range ADCP to our knowledge.

We found several datasets for which comparison of the time-averaged echo intensity profiles show poor agreement with the theoretical predictions given by Deines

Corresponding author address: Louis Gostiaux, Laboratoire des Écoulements Géophysiques et Industriels, LEGI/CORIOLIS, 21 rue des Martyrs, 38000 Grenoble, France.
E-mail: louis.gostiaux@legi.grenoble-inp.fr

DOI: 10.1175/2009JTECHO704.1

(1999), particularly in the tail of the profile when the backscattered intensity is less than one order of magnitude above the noise level. However, any quantitative study of backscattering strength variability is based on this comparison. A simple modification of Deines' equation that better fits with the data is the purpose of this letter.

2. Method

Propagation of sound in seawater is mainly affected by geometrical spreading, viscous dampening, and scattering by particles. This last effect is used by ADCPs, because the backscattered sound carries information on the velocity of the particles because of the Doppler effect. One may model the received intensity I from a signal initially emitted with an acoustic intensity I_0, transmitted along the acoustic beam over a distance R, and scattered back to the source as

$$I = I_0 \times \frac{10^{-(\alpha/10)R}}{R^2} \times \gamma R^2 s_v(R, t) \times \frac{10^{-(\alpha/10)R}}{R^2}, \qquad (1)$$

Here the second term on the right-hand side is spherical spreading and exponential attenuation between the transducer and the scatterer (α is the attenuation coefficient of sound in the media). The third term is backscattering by reflectors proportional to their volume backscattering strength s_v, which is a function of local concentration, cross section of the scatterer, and frequency of the acoustic signal; thus, it is a function of time and space. Note the γR^2 term to account for the spreading of the ensonified volume, with γ being a geometrical factor specific to the beam-pattern function and proportional to the transmit pulse length. The last term on the RHS is spherical spreading and exponential attenuation during the return path of the sound from the scatterer to the transducer.

A near-field correction can also be added, but it is not necessary in this study. Expressed in decibels [$I_{\mathrm{dB}} = 10\log(I/I_{\mathrm{ref}})$, with I_{ref} being an arbitrary reference intensity level] and introducing a constant A that incorporates I_0 and the time- and distance-independent coefficients, (1) (in decibels) becomes

$$I_{\mathrm{dB}} = A - 20\log(R) - 2\alpha R + 10\log[s_v(R, t)], \qquad (2)$$

where A is independent of time and space. Using this equation, relative backscattering strength (in decibels, to a distance R_0) can be computed as

$$10\log\frac{s_v(R, t)}{s_v(R_0, t)} = I_{\mathrm{dB}}(R, t) - I_{\mathrm{dB}}(R_0, t) + 20\log\frac{R}{R_0} + 2\alpha(R - R_0). \qquad (3)$$

This relation is used to calibrate ADCP data with simultaneous water samples or OBS measurements that can provide an estimate of $s_v(R_0)$ at a given time t_0. When the temporal and spatial variations of s_v are due to concentration changes only, the relative concentrations of scatterers can be computed the same way. However, we would like to emphasize that, although (2) is true as for acoustic intensity, systematic errors occur when this expression is applied directly to the measured ADCP backscattered intensity.

This is due to the fact that the Teledyne RD Instruments Co. (RDI) ADCP received signal strength indicator (RSSI) is a logarithmic measure of the acoustic intensity in the water. A scale factor k_c is used to convert RSSI counts to decibels (RDI 2001). The ADCP records both the backscattered signal and the ambient noise of the water in its receiving band. Thus, in the presence of noise, we have (in decibels)

$$k_c E = 10\log\left(\frac{I + I_{\mathrm{noise}}}{I_{\mathrm{ref}}}\right), \qquad (4)$$

where E is the RSSI, I_{noise} is the acoustic intensity of the noise, and I_{ref} is a reference intensity imposed by the hardware. The precise determination of k_c is crucial if any quantitative measurement is to be done, because fluctuations of 20% are observed around the commonly used value of $k_c = 0.45$ (Deines 1999) and also between the individual transducers of a single ADCP.

However, the main error remains if the noise level is neglected when combining (1) and (4). Indeed, if we define $E_{\mathrm{noise}} = (10/k_c)\log(I_{\mathrm{noise}}/I_{\mathrm{ref}})$ as the noise level in counts, we have (in decibels)

$$10\log(10^{k_c E/10} - 10^{k_c E_{\mathrm{noise}}/10}) = I_{\mathrm{dB}}. \qquad (5)$$

Because $\log(x + y) \neq \log x + \log y$, this expression obviously differs from the statement $k_c(E - E_{\mathrm{noise}}) = I_{\mathrm{dB}}$. It is surprising that in the work of Deines (1999) this problem, although briefly mentioned in one equation of the appendix, is not included in the final expression for backscatter strength. If we literally reproduce here from Deines [(1999), Eq. (A-5)] the expression

$$\frac{S + N}{N} = 10\log\left[\frac{k_c(E - E_r)}{10}\right], \text{ (uncorrected)}, \qquad (6)$$

where S is the backscattered signal power, N is the noise power, and $E_r = E_{\mathrm{noise}}$, and correct it for an unfortunate typing error as follows,

$$\frac{S + N}{N} = 10^{k_c(E - E_r)/10}, \text{ (corrected)}, \qquad (7)$$

we have a rigorous introduction of N in the signal-to-noise ratio because the power recorded by the ADCP is indeed $S + N$. However, because the sonar equation in (A-1) proposed by Deines (1999) gives the theoretical value of the ratio S/N, we see that, to identify S/N with $(S + N)/N$, the assumption $S + N \simeq S$ was made by the author without being mentioned. This is not obvious, because the author suggests that $E_r = E_{\text{noise}}$ can be estimated at the tail (large R) of the profile (where thus $S \simeq N$). We will show in the following how the above error modifies the estimation of absolute backscattering strength as well as relative concentration estimates, when $S/N \leq 10$, that is, for $k_c(E - E_{\text{noise}}) < 10$.

Following (5), we propose to model the evolution of E (RSSI counts) along R in an ADCP beam as (in decibels)

$$10 \log(10^{k_c E/10} - 10^{k_c E_{\text{noise}}/10}) = A - 20 \log(R) - 2\alpha R + 10 \log[s_v(R, t)]. \tag{8}$$

This equation can be used for estimates of the absolute backscatter strength, provided the constant A is determined using the set of formulas proposed by Deines (1999). It can also be used to estimate relative backscatter strength or relative backscatter concentration for which the determination of A is not needed.

3. Observations

We found several datasets for which we needed to remove noise levels in arithmetic space to have a satisfying matching between observation and theory. We applied our equation to the time-averaged intensity profiles for each dataset, assuming that the time (logarithmic) average of the backscattering strength was a constant relative to R. Doing so, $\langle \log(s_V) \rangle_t$ can be incorporated in the constant A, and the time-averaged RSSI curves can be fitted with (9):

$$k_c \overline{E} = 10 \log\{10^{[A - 20\log(R) - 2\alpha R]/10} + 10^{k_c E_{\text{noise}}/10}\} \quad \text{NEW}$$

and (9)

$$k_c \overline{E} = A - 20 \log(R) - 2\alpha R + k_c E_{\text{noise}} \quad \text{OLD}. \tag{10}$$

For comparison, we reproduce (10) inferred from Deines (1999). In Fig. 1a, it is shown how (9) and (10) diverge as E approaches E_{noise} to within 10 dB. In the case $E > E_{\text{noise}} + 10$, the uncorrected (10) can be used, however, with a 0.5-dB confidence interval. This is consistent with an observation in Zedel (2001) of the lowest significant sound levels resolved by an ADCP.

In (9), α is estimated using Schulkin and Marsh equations as proposed by Urick (1975), and correction for the attenuation by the scatterers themselves can be neglected in first approximation, because we are not working with frequencies larger than 10^6 Hz (Gartner 2004), except for one dataset using a 1200-kHz ADCP (limit case). The term E_{noise} is the tail value of the minimum RSSI profile over the total record. Because the RSSI counts are integers and we take the minimum of this value over long time series, we allow ourselves to add an adjustable constant δE_{noise} to E_{noise} that ranges between 0 and 1 to compensate for this discretization. For an ADCP with beams slanted at an angle θ to the vertical, range R is computed from

$$R = \frac{R_1 + D/4 + (n - 1)D}{\cos\theta}, \tag{11}$$

where R_1 is the distance to the center of the first bin, n is the vertical bin number, and D is the size of a depth cell. All of these variables are provided in the RDI ADCP fixed leader data, and we checked that the first bin distance is computed using $R_1 = B + (L + D + \text{La})/2$, where B is the blanking distance, L is the transmit pulse length, and La is the transmit lag. This expression differs from Deines [(1999), Eq. (3)], where the transmit lag distance is not included.

Scale factor k_c and constant A are adjusted to obtain the best fit of (9) with the data, with k_c being constrained to the range [0.35, 0.55]. However, it can be shown that, when following Deines (1999), no value of A and k_c can be found that gives a correct fit along the profile. Using the correct (9), deviation of the time-averaged profiles from (9) can now be interpreted as spatial (depth) variations of the time-averaged backscattering strength $\overline{s}_v$.

The different datasets from which Figs. 1–f are obtained are presented in Table 1. An inset plot with the RSSI distance–time series also is visible in Fig. 1 for each dataset. We have the following five datasets:

1) Astronomy with a Neutrino Telescope and Abyss Environmental Research (ANTARES): This ADCP is part of the ANTARES neutrino telescope that directly sends information to the coast using the submarine network developed for cosmic particle detection. It is downward looking in the deep Mediterranean Sea waters at a depth of 2300 m. The RSSI values are very weak and do not show strong backscattering variability (J. A. Aguilar 2010, manuscript submitted to *Geophys. Res. Lett.*).
2) Processes above Continental Slopes (PROCS): The ADCP mooring was part of an extensive multidisciplinary program to study the effects of internal wave–induced mixing on sediment transport and nutrient

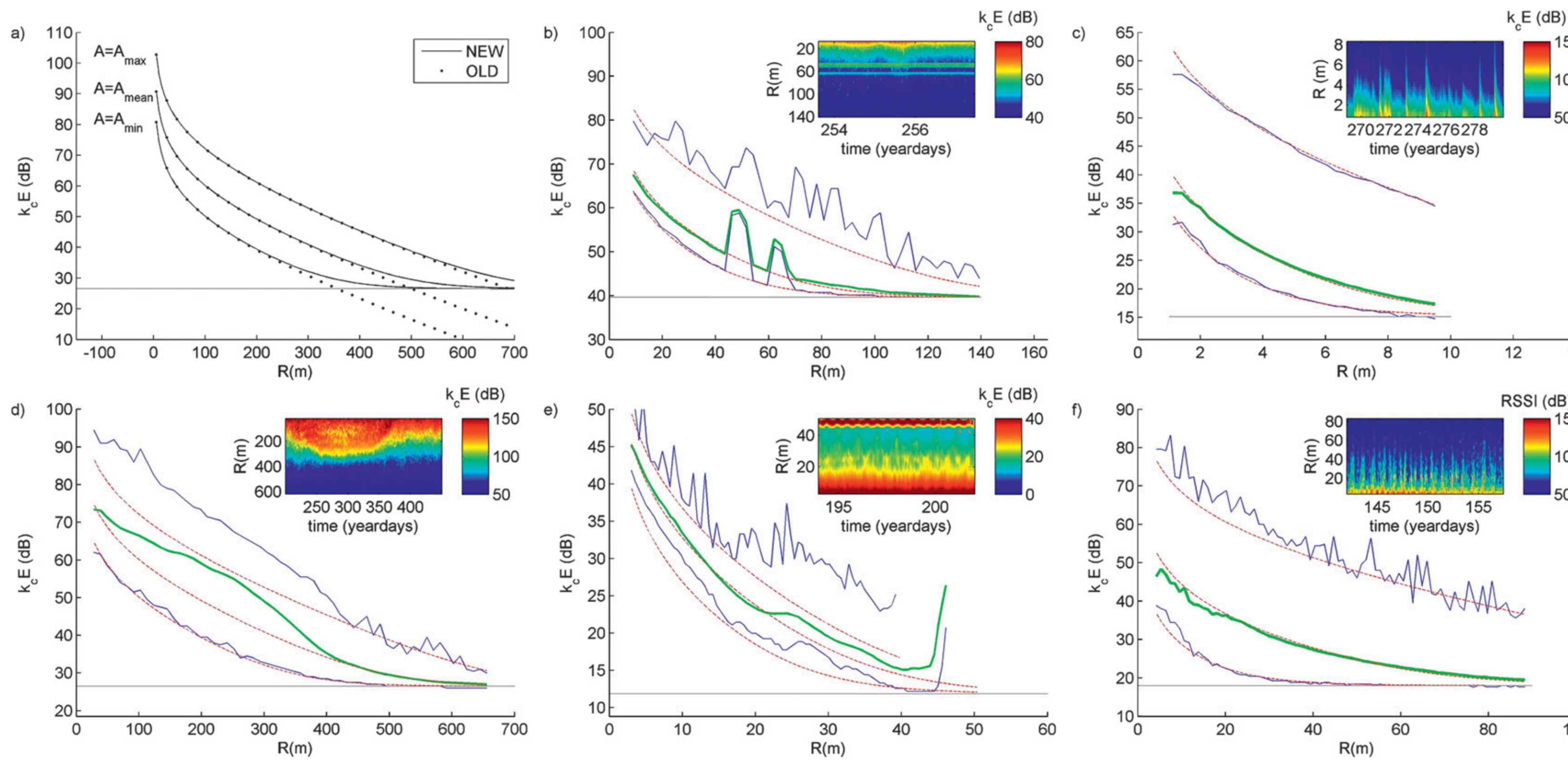

FIG. 1. (a) Comparison of the intensity profiles computed using (9) and (10): the new equation proposed in this study (solid line) and the one obtained following Deines (1999; dots); α and k_cE_{noise} (gray line) correspond to the case 3 in Table 2, and the three curves correspond to $A = A_{\mathrm{min}}$, A_{mean}, and A_{max}. Shown in (b)–(f) are comparisons between the measured and theoretical RSSI profiles: the minimum and maximum RSSI profiles (blue line), the time-averaged RSSI values using a geometric average (green line), and the results from (9) with the parameters listed in Table 2 that fit best with the minimum, geometrically averaged, and maximum profiles (dotted red lines). The horizontal gray line represents $E = E_{\mathrm{noise}} + \delta E_{\mathrm{noise}}$. A distance–time series of the RSSI data is shown in the insets, with the ordinate axis being correctly oriented. The datasets used are (b) ANTARES, where the anomalous data around R = 48 and 63 m are due to reflections on other instruments; (c) PROCS; (d) LOCO; (e) INP, where the red band for $R > 40$ m corresponds to data beyond the water surface; and (f) DOC. Note that the axis scales are different.

TABLE 1. Observation details of moored Teledyne RDI ADCPs. Temperature T is measured by the ADCP, and here salinity is designated by S in parts per thousand and is estimated from corresponding CTD profiles at the depth of the instrument. Start and end dates indicate portions of the time series used.

No.	Name	Start date	End date	Lat	Lon	Depth (m)	T (°C)	S (ppt)
1	ANTARES	10 Sep 2006	14 Sep 2006	42°48.00N	06°10.00E	2469	13.0	38.5
2	PROCS	27 Sep 1999	8 Oct 1999	60°51.06N	02°58.01W	500	6.7	34.9
3	LOCO	2 Jul 2006	27 Mar 2007	33°00.01N	22°24.41W	1350	7.2	36.1
4	INP	13 Jul 1994	22 Jul 1994	54°25.00N	04°02.00E	45	9	34.5
5	DOC	24 May 2006	31 May 2006	30°00.05N	28°18.80W	540	13.2	35.6

redistribution on the continental slope of the Faeroe–Shetland Channel. The upward-looking ADCP was mounted in a bottom frame to which a thermistor string was attached. The echo data ranged between 0.9 and 8.15 m above the bottom and hence are affected by sediment resuspension (Hosegood and van Haren 2004).

3) Long-Term Ocean Climate Observations (LOCO): On this long-term mooring (530 days in total), the ADCP was mounted in the top buoy, downward-looking from a depth of 1400 m to 2000 m in the central part of the Canary Basin. Total water depth is 5270 m. Most of the backscattering is due to living organisms that move up and down with diurnal periodicity (van Haren 2007b).
4) Integrated North Sea Program (INP): This is an ADCP upward looking from the seafloor (45 m) to the surface in the shallow North Sea. Backscatterers are a combination of sediments, air bubbles, and zooplankton (van Haren et al. 1999).
5) Deep Ocean Current (DOC): The ADCP was attached to a bottom lander on the eastern slope of the Great Meteor Seamount to monitor internal wave breaking and fronts. Echo data range from 4 to 80 m above bottom and reveal zooplankton migration at the solar diurnal constituent (S1) modulated by the internal tide (M2; van Haren 2009).

Figures 1b–f show for each dataset the minimum, maximum, and geometrically averaged RSSI profiles over a specific time interval of the complete time series. This interval is chosen so as to highlight specific phenomena in the distance–time series visible in the inset. For each dataset, our equation fits the main trend of the different profiles. The only parameter changing among the three profiles for a given dataset is the constant A (see Table 2 for the values of the different parameters A_{min}, A_{mean}, and A_{max}). There are, of course, deviations from the theoretical profile, but these are precisely the variation along R of the minimum, maximum, or time-averaged backscattering strength that we want to investigate. This demonstrates that finding the best theoretical model is very important to estimate these variations. There is, as a validation of (9), only a very small mismatch between constant backscattering strength theory and observations for the ANTARES data (Fig. 1b), which reflects the strong homogeneity of the deep Mediterranean waters.

4. Discussion

We propose a simple modification to the equations proposed by (Deines 1999), in which we subtract the noise level in arithmetic space for a correct use of the sonar equation in logarithmic space. Our equation fits the time-averaged RSSI data from very different datasets up to the tail of each profile, whereas if we followed Deines (1999) we would observe a divergence when the signal goes below 10 times the noise level. For the present datasets, this accounts for half of the ADCP range, which is of course a substantial improvement. The above bias was probably not taken into account (yet being possibly significant) when only the relative backscattering

TABLE 2. Acoustic details for the various ADCPs of Table 1. All are RDI four-beam instruments. Approximate transmit frequency is denoted by F. Data can be beam dependent and are computed for beam 1. See text for other symbols.

No.	Type	F (kHz)	Orientation	α (dB km^{-1})	k_c (dB counts^{-1})	$k_c E_{\mathrm{noise}}$ (dB)	A_{min} (dB)	A_{mean} (dB)	A_{max} (dB)
1	Workhorse	300	Down	77.3	0.55	39.6	84	89	103
2	Broadband	1200	Up	512	0.36	15.1	35	42	64
3	Long Ranger	75	Down	24.5	0.5	26.5	95	105	117
4	Broadband	600	Up	163	0.37	11.8	50	56	60
5	Workhorse	300	Up	82.6	0.4	18.0	50	66	90

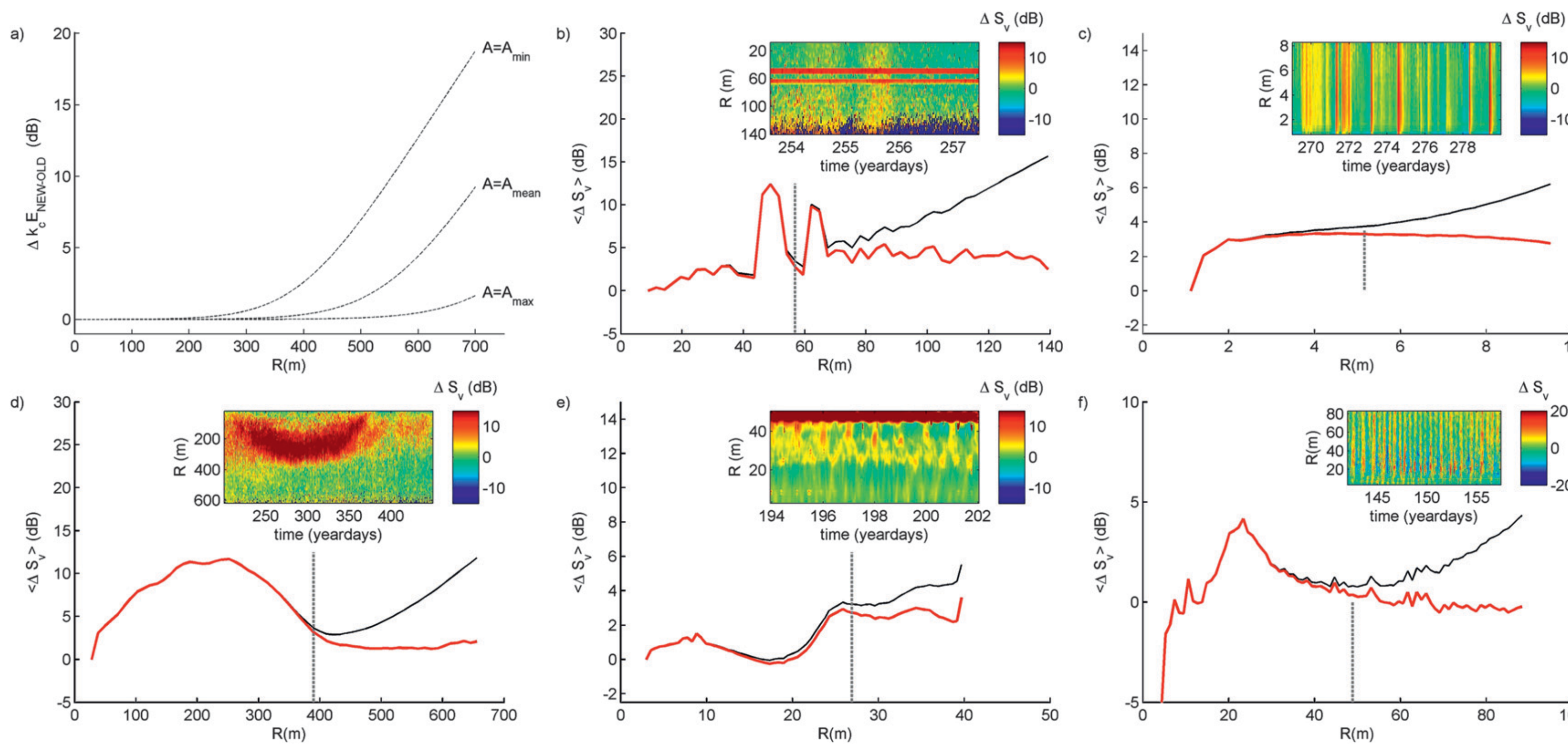

FIG. 2. (a) Difference between the intensity profiles computed using (9) and (10), as in Fig. 1a: This difference will appear in (3) and will artificially increase s_v. Shown in (b)–(f) are relative backscattering strength s_v computed using the combination of (3) and (5) (red) and following Deines (1999; black) for the same datasets as in Fig. 1. The vertical gray dashed line shows the distance at which the threshold $10E_{\text{noise}}$ is attained. In the insets, the time–distance series of ΔS_v over the selected range is shown. The datasets used are (b) ANTARES, (c) PROCS, (d) LOCO, (e) INP, and (f) DOC. Note that the axis scales are different.

strength profiles are plotted. It results in a systematic overestimate of the backscattering strength at the tail of the profile (see Fig. 2a).

In Figs. 2b–f, we show for the previous datasets the relative backscattering strength $S_v = 10\log[s_v(R)/s_v(R_0)]$, where R_0 is arbitrarily chosen as the first significant bin distance. The choice of R_0 only translates the profiles vertically above or below 0. In the inset distance–time series, after subtracting the theoretical profile, different kind of backscatterers can then be observed and their relative strength can be quantified. In Fig. 2b, a very weak backscattering strength variation is thus observed in deep (2300 m) homogeneous Mediterranean waters, which has inertial periodicity. In Fig. 2c, backscattering is dominated by very intense short-term increases resulting from sediment resuspended by upslope moving solitary bores that are also distinguished in the velocity data. In Fig. 2d, there is a strong seasonal plankton migration over a 100-m range. In Fig. 2e, the range of the V-shaped planktonic migration down to 20 m below the sea surface is clearly visible. In Fig. 2f, the initially S1-dominant signal of zooplankton migration is altered when the vertical velocity of the M2 internal tide is in the opposite direction to the animals' displacement. Our improvement is thus useful to correctly interpret RSSI data in these different conditions and for any quantitative observation based on echo intensity data approaching the noise level by a factor of 10.

Acknowledgments. The assistance of the crew of R/V *Pelagia* is highly appreciated. We thank Theo Hillebrand for assistance in mooring preparation and handling. We acknowledge the ANTARES collaboration for the use of the ADCP dataset (available online at http://antares.in2p3.fr/). Integrated North Sea Program (INP), Processes above Continental Slopes (PROCS), and Long-Term Ocean Climate Observations (LOCO) were funded in part by the Netherlands Organization for the Advancement of Scientific Research (NWO). Author Gostiaux was funded in part via BSIK.

REFERENCES

Betteridge, K., P. Thorne, and R. Cooke, 2008: Calibrating multi-frequency acoustic backscatter systems for studying near-bed suspended sediment transport processes. *Cont. Shelf Res.,* **28,** 227–235.

Deines, K. L., 1999: Backscatter estimation using broadband acoustic Doppler current profilers. *Proc. Sixth Working Conf. on Current Measurement,* San Diego, CA, IEEE, 249–253.

Flagg, C. N., and S. L. Smith, 1989: On the use of the acoustic Doppler current profiler to measure zooplankton abundance. *Deep-Sea Res.,* **36,** 455–474.

Gartner, J. W., 2004: Estimating suspended solids concentrations from backscatter intensity measured by acoustic Doppler current profiler in San Francisco Bay, California. *Mar. Geol.,* **211,** 169–187.

Hosegood, P., and H. van Haren, 2004: Near-bed solibores over the continental slope in the Faeroe-Shetland Channel. *Deep-Sea Res. II,* **51,** 2943–2971.

Kim, Y. H., and G. Voulgaris, 2003: Estimation of suspended sediment concentration in estuarine environments using acoustic backscatter from an ADCP. *Proc. Fifth Int. Conf. on Coastal Sediments,* Clearwater Beach, FL, World Scientific Corporation, CD-ROM.

Plueddemann, A. J., and R. Pinkel, 1989: Characterization of the patterns of diel migration using a Doppler sonar. *Deep-Sea Res.,* **36,** 509–530.

RDI, 2001: Workhorse commands and output data format. RD Instruments Tech. Rep. 957-6156-00, 158 pp.

Urick, R. J., 1975: *Principles of Underwater Sound*. McGraw-Hill, 384 pp.

van Haren, H., 2007a: Echo intensity data as a directional antenna for observing processes above sloping ocean bottoms. *Ocean Dyn.,* **57,** 135–149.

——, 2007b: Monthly periodicity in acoustic reflections and vertical motions in the deep ocean. *Geophys. Res. Lett.,* **34,** L12603, doi:10.1029/2007GL029947.

——, 2009: Using high sampling-rate ADCP for observing vigorous processes above sloping [deep] ocean bottoms. *J. Mar. Syst.,* **77,** 418–427, doi:10.1016/j.jmarsys.2008.10.012.

——, L. Maas, J. Zimmerman, H. Ridderinkhof, and H. Malschaert, 1999: Strong inertial currents and marginal internal wave stability in the central North Sea. *Geophys. Res. Lett.,* **26,** 2993–2996.

Wall, G., E. Nystrom, and S. Litten, 2006: Use of an ADCP to compute suspended-sediment discharge in the tidal Hudson River, New York. U.S. Geological Survey Scientific Investigations Rep. 5055, 26 pp.

Zedel, L., 2001: Using ADCP background sound levels to estimate wind speed. *J. Atmos. Mar. Technol.,* **18,** 1867–1881.